JACS
JOURNAL OF THE AMERICAN CHEMICAL SOCIETY

ARTICLE

pubs.acs.org/JACS

Comproportionation of Cationic and Anionic Tungsten Complexes Having an *N*-Heterocyclic Carbene Ligand To Give the Isolable 17-Electron Tungsten Radical $CpW(CO)_2(IMes)^{\bullet}$

John A. S. Roberts,[†] James A. Franz,[†,§] Edwin F. van der Eide,[†] Eric D. Walter,[†] Jeffrey L. Petersen,[‡] Daniel L. DuBois,[†] and R. Morris Bullock*[,†]

[†]Chemical and Materials Sciences Division, Pacific Northwest National Laboratory, P.O. Box 999, K2-57, Richland, Washington 99352, United States

[‡]C. Eugene Bennett Department of Chemistry, West Virginia University, Morgantown, West Virginia 26506-6045, United States

Supporting Information

ABSTRACT: A series consisting of a tungsten anion, radical, and cation, supported by the *N*-heterocyclic carbene 1,3-bis-(2,4,6-trimethylphenyl)imidazol-2-ylidene (IMes) and spanning formal oxidation states W(0), W(I), and W(II), has been synthesized, isolated, and characterized. Reaction of the hydride $CpW(CO)_2(IMes)H$ with KH and 18-crown-6 gives the tungsten anion $[CpW(CO)_2(IMes)]^-[K(18\text{-crown-}6)]^+$. Electrochemical oxidation of $[CpW(CO)_2(IMes)]^-$ in MeCN (0.2 M $^nBu_4N^+PF_6^-$) is fully reversible ($E_{1/2} = -1.65$ V vs $Cp_2Fe^{+\bullet/0}$) at all scan rates, indicating that $CpW(CO)_2(IMes)^{\bullet}$ is a persistent radical. Hydride transfer from $CpW(CO)_2(IMes)H$ to $Ph_3C^+PF_6^-$ in MeCN affords $[cis\text{-}CpW(CO)_2(IMes)(MeCN)]^+PF_6^-$. Comproportionation of $[CpW(CO)_2(IMes)]^-$ with $[CpW(CO)_2(IMes)(MeCN)]^+$ gives the 17-electron tungsten radical $CpW(CO)_2(IMes)^{\bullet}$. This complex shows paramagnetically shifted resonances in the ^1H NMR spectrum and has been characterized by IR spectroscopy, low-temperature EPR spectroscopy, and X-ray diffraction. $CpW(CO)_2(IMes)^{\bullet}$ is stable with respect to disproportionation and dimerization. NMR studies of degenerate electron transfer between $CpW(CO)_2(IMes)^{\bullet}$ and $[CpW(CO)_2(IMes)]^-$ are reported. DFT calculations were carried out on $CpW(CO)_2(IMes)H$, as well as on related complexes bearing NHC ligands with N,N′ substituents Me ($CpW(CO)_2(IMe)H$) or H ($CpW(CO)_2(IH)H$) to compare to the experimentally studied IMes complexes with mesityl substituents. These calculations reveal that W−H homolytic bond dissociation energies (BDEs) decrease with increasing steric bulk of the NHC ligand, from 67 to 64 to 63 kcal mol^{-1} for $CpW(CO)_2(IH)H$, $CpW(CO)_2(IMe)H$, and $CpW(CO)_2(IMes)H$, respectively. The calculated spin density at W for $CpW(CO)_2(IMes)^{\bullet}$ is 0.63. The W radicals $CpW(CO)_2(IMe)^{\bullet}$ and $CpW(CO)_2(IH)^{\bullet}$ are calculated to form weak W−W bonds. The weakly bonded complexes $[CpW(CO)_2(IMe)]_2$ and $[CpW(CO)_2(IH)]_2$ are predicted to have W−W BDEs of 6 and 18 kcal mol^{-1}, respectively, and to dissociate readily to the W-centered radicals $CpW(CO)_2(IMe)^{\bullet}$ and $CpW(CO)_2(IH)^{\bullet}$.

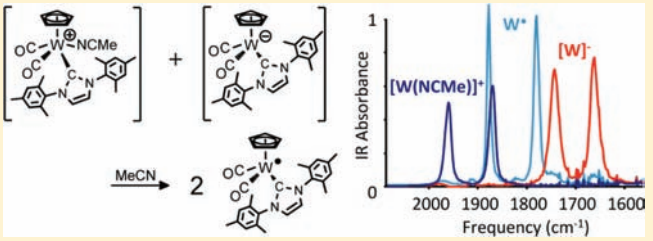

INTRODUCTION

The importance of 17-electron metal radicals is now well-recognized.[1,2] Highly reactive $Cp(CO)_3Mo^{\bullet}$ and $Cp(CO)_3W^{\bullet}$ are produced by photochemical homolysis of the M−M bonded dimers $[Cp(CO)_3M]_2$.[3] Tyler and co-workers reported extensive studies of the reactions of $Cp(CO)_3Mo^{\bullet}$ with phosphines, resulting in disproportionation proceeding through 19-electron intermediates.[4] $Cp(CO)_3W^{\bullet}$ and related radicals can also abstract halogen atoms from halogenated hydrocarbons, and rate constants for many such reactions have been reported.[5,6] In the absence of reactive substrates, these metal-centered radicals dimerize at (or close to) diffusion-controlled rates, with dimerization rate constants typically around 3×10^9 M^{-1} s^{-1}.[3,5,7] Reactions of the radicals $Cp(CO)_3Mo^{\bullet}$[8] and $Cp(CO)_3W^{\bullet}$[9] have been observed by time-resolved IR spectroscopy, and recent studies have used ultrafast spectroscopy and two-dimensional IR to study their reactivity.[10] The M−M bonded dimers $[Cp(CO)_3M]_2$ (M = Mo, W) do not thermally homolyze to $Cp(CO)_3M^{\bullet}$ to an appreciable extent; $\Delta G^{o\prime} = 22 \pm 3$ kcal mol^{-1} for homolysis of the Mo−Mo bond in $[Cp(CO)_3Mo]_2$.[11] In contrast, Tyler and co-workers found that $[(C_5Ph_5)Mo(CO)_3]_2$, having a bulky pentaphenyl-substituted Cp ring, undergoes Mo−Mo bond dissociation to a greater extent.[12]

The Cr−Cr bond in $[Cp(CO)_3Cr]_2$ is weaker than the analogous Mo−Mo or W−W bonds, and the 17-electron radical $Cp(CO)_3Cr^{\bullet}$ is in equilibrium with the dimer.[13,14] The chromium radical $Cp(CO)_3Cr^{\bullet}$ has been found to dimerize at somewhat less than diffusion-controlled rate constants ($k = 3 \times 10^8$ M^{-1} s^{-1}),[15] making it more persistent[16] than its Mo

Received: March 26, 2011
Published: July 22, 2011

and W congeners. The chromium radical $Cp(CO)_3Cr^{\bullet}$ and related derivatives have shown useful organic reactivity, particularly for radical cyclization reactions involving chain-transfer catalysis.[17] Substitution of one CO with a phosphine ligand increases the stability of the Cr radical, and chromium radicals such as $Cp(CO)_2(PPh_3)Cr^{\bullet}$ have been isolated.[14,18]

Compared to first-row metals such as chromium, third-row metals like tungsten generally form stronger bonds to other metals and to carbon or hydrogen. Whereas the piano-stool complex $Cp(CO)_3W^{\bullet}$ is very reactive, a handful of W(I) and W(V) 17-electron complexes are sufficiently stable to be isolated. Examples of W(I) radicals include $Tp^*W(CO)_3^{\bullet}$ ($Tp^* = \kappa^3$-*N*-hydridotris(3,5-dimethylpyrazolyl)borate),[19] $(CO)_3(P^iPr_3)_2$-$WI^{\bullet}$,[20] and $Tp^*W(CO)_2(\eta^2\text{-}RC{\equiv}CR')^{\bullet}$ (R = R′ = Ph or Me; R = Ph, R′ = H).[21] Odd-electron W(V) complexes include the trihydride complex $Cp^*W(dppe)H_3^{\bullet+}PF_6^-$ (dppe = bis(diphenylphosphino)ethane),[22] the methylidyne $[(Me_3P)_4W(Cl){\equiv}CH]^{+\bullet}B(C_6F_5)_4^-$,[23] $Cp_2WCl_2^{+\bullet}$,[24] and naturally occurring tungstoenzymes.[25]

N-Heterocyclic carbenes (NHCs) are versatile,[26] and several examples of paramagnetic NHC complexes exist. Danopoulos and co-workers have reported paramagnetic complexes of Fe,[27] Co,[28] and V[29] having pincer pyridine dicarbene (CNC) ligands. Meyer and co-workers prepared paramagnetic tris-carbene complexes of Ni,[30] Co,[31] and Cu.[32] Several paramagnetic Ni(II) complexes that bear multidentate NHC ligands are known.[33] These complexes have NHC ligands as a part of a *multidentate* ligand set, but there are also a few examples of paramagnetic complexes that have a *monodentate* ligand such as 1,3-bis(2,4,6-trimethylphenyl)imidazol-2-ylidene (IMes), a prototypical, widely used NHC. The Mo complex $CpMo(CO)_2(IMes)^{\bullet}$ was prepared by a photochemical route and was characterized only by electron paramagnetic resonance (EPR) spectroscopy.[34] First-row metals that form paramagnetic complexes with IMes ligands include Ti(III),[35] V(III),[36] Mn(I),[37] Fe(II),[38] and Ni(I).[39] These examples show that paramagnetic complexes containing NHC ligands are most common for *first-row metals* and often have multidentate ligands.

We report here the synthesis and structure of the tungsten anion $[CpW(CO)_2(IMes)]^-$. Electrochemical or chemical oxidation of $[CpW(CO)_2(IMes)]^-$, or comproportionation of $[CpW(CO)_2(IMes)]^-$ with $[CpW(CO)_2(IMes)(MeCN)]^+$, provides the 17-electron radical $CpW(CO)_2(IMes)^{\bullet}$, a rare example of a stable third-row metal radical with an NHC ligand. This complex was characterized by NMR, EPR, and IR spectroscopy and X-ray crystallography. A computational treatment sheds light on the origins of the stability of the radical.

RESULTS AND DISCUSSION

Synthesis and Characterization of $[CpW(CO)_2(IMes)]^-[K(18\text{-crown-6})]^+$. No visible change occurs when $CpW(CO)_2(IMes)H$ is stirred with KH in THF, but deprotonation proceeds rapidly with gas evolution when a THF solution of 18-crown-6 is added, leading to the isolation of highly crystalline orange needles (eq 1). This reaction is based on extensive work by Morris and co-workers, who have isolated a considerable variety of transition metal anions as $K(crypt)^+$ and $K(crown)^+$ salts from reactions of KH with neutral metal species in the presence of a crown ether or a cryptand.[40,41]

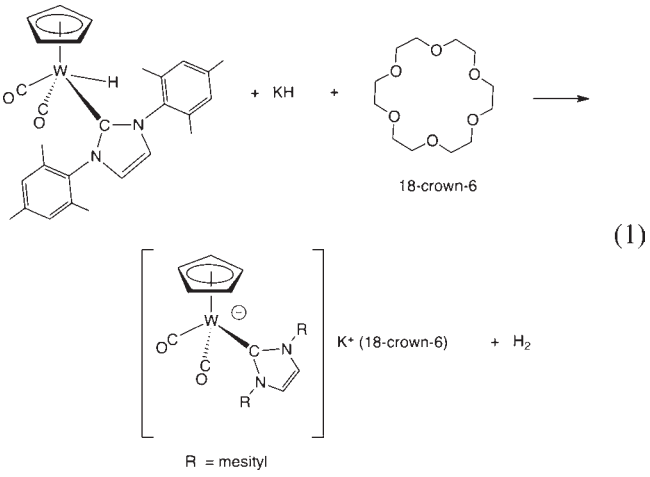

(1)

The ^{1}H NMR spectrum of $[CpW(CO)_2(IMes)]^-[K(18\text{-crown-6})]^+$ at 20 °C in THF-d_8 shows broadened IMes resonances, with one signal for each of the IMes aryl (*o*-Me, *m*-H, and *p*-Me) substituents and one for the vinyl protons. Equivalence across the plane bisecting the IMes ligand (signal 1 = 1′ and 2 = 2′ in Scheme 1) indicates that the anion adopts C_s symmetry on the NMR time scale. Furthermore, equivalence of all of the *o*-Me protons and all of the aromatic protons suggests that fast rotation about the $W{-}C_{IMes}$ bond occurs. As illustrated in Scheme 1 for the *o*-Me groups, a 180° rotation will exchange 1 with 2′ and 1′ with 2. Together with the C_s symmetry, this results in 1 = 1′ = 2 = 2′.

Scheme 1

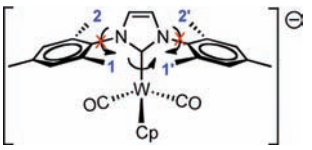

Although rotation about the $C{-}N_{Mes}$ bond would, in principle, be able to exchange 1 with 2 and 1′ with 2′ to also render all *o*-Me groups equivalent, barriers for such mesityl rotations in metal complexes with IMes ligands are at least 30 kcal mol^{-1},[42] which means that mesityl rotations are extremely slow on the NMR time scale. Variable-temperature NMR studies in other systems have also shown that $M{-}C_{IMes}$ rotation is fast relative to $C{-}N_{Mes}$ rotation.[43]

The ^{1}H NMR chemical shifts of $[CpW(CO)_2(IMes)]^-[K(18\text{-crown-6})]^+$ in THF-d_8 are only moderately temperature-dependent over the range from −60 to 20 °C, with broadening of the *m*-H (3.8 → 5.4 Hz) and *o*-Me signals (2.0 → 3.7 Hz) at reduced temperatures. Considerable narrowing of the vinyl (∼34 → 4.7 Hz) and *p*-Me signals (13.4 → 6.2 Hz) and to a lesser degree the Cp resonance (7.4 → 4.9 Hz) is observed at lower temperatures.

In light of the strong reducing character of $[CpW(CO)_2(IMes)]^-$, its reversible oxidation electrochemistry (see below), and the unexpected response of signal widths to lower temperature, we hypothesized that trace amounts of the 17-electron radical $CpW(CO)_2(IMes)^{\bullet}$ are in rapid electron-transfer

exchange with $[CpW(CO)_2(IMes)]^-$. To assess this possibility, a drop of sodium−potassium alloy (NaK) was added to a THF-d_8 solution of $[CpW(CO)_2(IMes)]^-[K(18\text{-crown-6})]^+$ to reduce any $CpW(CO)_2(IMes)^\bullet$ that might be present. This had little effect on chemical shifts (0.02 ppm or less) but a dramatic effect on line widths, narrowing the Cp, *p*-Me, and vinyl resonances (7.4 → 0.7 Hz, 13.4 → 6.3 Hz, and 34 → 0.6 Hz, respectively) and broadening the *m*-H and *o*-Me resonances (3.8 → 5.9 Hz and 2.0 → 9.4 Hz). The NMR data point to a superposition of rapid rotational isomerization in $[CpW(CO)_2(IMes)]^-$ and degenerate electron transfer between $[CpW(CO)_2(IMes)]^-$ and trace amounts of $CpW(CO)_2(IMes)^\bullet$.

The solution IR spectrum of $[CpW(CO)_2(IMes)]^-[K(18\text{-crown-6})]^+$ exhibits ν_{CO} bands at unusually low energy for terminal CO ligands (1743 and 1662 cm^{-1} in MeCN, and 1765 and 1664 cm^{-1} in THF). For comparison, Norton and co-workers reported ν(CO) bands for $[CpW(CO)_2(PMe_3)]^-K^+$ at 1762 and 1682 cm^{-1} in MeCN,[44] suggesting that the IMes ligand is an exceptionally strong electron donor, even compared to strongly donating PMe_3. This property is examined in further detail in a comparison of the thermochemistry of W−H bonding of $CpW(CO)_2(PMe_3)H$ and $CpW(CO)_2(IMes)H$.[45,46]

Structure of $[CpW(CO)_2(IMes)]^-[K(18\text{-crown-6})]^+$. The structure of the tungsten anion complex was determined by single-crystal X-ray diffraction (XRD) and is shown in Figure 1. The anion $[CpW(CO)_2(IMes)]^-$ assumes a three-legged piano-stool configuration wherein the plane defined by the Cp-centroid, the W atom, and the carbene carbon roughly bisects the C_{CO}−W−C_{CO} angle.

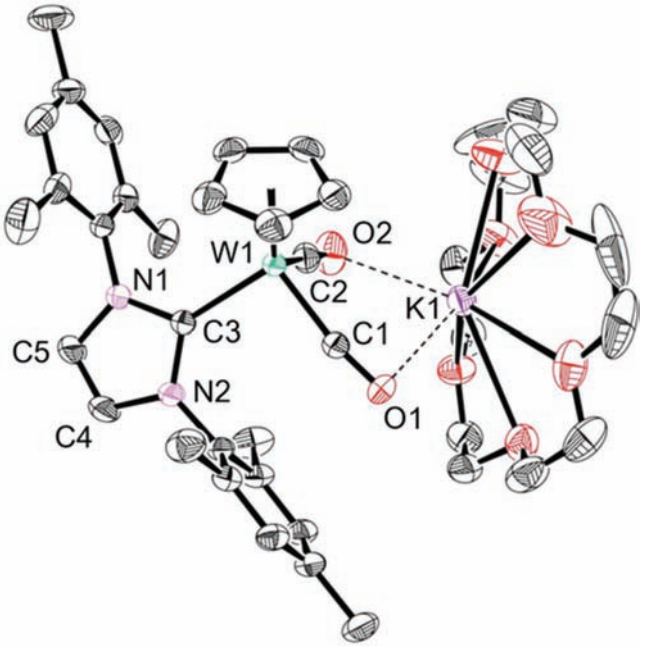

Figure 1. Molecular structure of $[CpW(CO)_2(IMes)]^-[K(18\text{-crown-6})^+]$. The crown ether bound to K^+ suffers from a 2:1 orientation disorder (major component shown). Ellipsoids are plotted at the 30% confidence level. Selected bond lengths (Å) and angles (°): W(1)−C(1) 1.907(2), W(1)−C(2) 1.901(3), W(1)−C(3) 2.131(2), C(1)−O(1) 1.198(3), C(2)−O(2) 1.197(3), $Cp_{centroid}$−W(1) 2.035(1), O(1)−K(1) 2.824(2), O(2)−K(1) 3.062(2); C(1)−W(1)−C(2) 85.61(11), C(1)−W(1)−C(3) 95.86(9), C(2)−W(1)−C(3) 93.63(10), W(1)−C(1)−O(1) 171.3(2), W(1)−C(2)−O(2) 174.5(2), C(1)−O(1)−K(1) 87.93(15), C(2)−O(2)−K(1) 83.24(18).

In contrast, the hydride $CpW(CO)_2(IMes)H$ exhibits carbonyl positions that are distinctly *cis* and *trans* with respect to the carbene ligand.[47] Because of the lower coordination number, the C_{CO}−W−C_{CO} angle is larger in the anion (85.61(11)°) than in the hydride (77.7(2)°). The W−C_{CO} bond lengths (1.907(2) and 1.901(3) Å) are shorter than those in the hydride $CpW(CO)_2(IMes)H$ (1.927(5) and 1.936(6) Å) because of the larger amount of W(d)−CO(π^*) backbonding in the anion; for the same reason, long C−O bonds of ca. 1.20 Å are observed. An even larger difference is found in the W−$C_{carbene}$ distance for the anion (2.131(2) Å) vs that found in the hydride (2.183(5) Å). Differences between these two species in IMes imidizole C−C and C−N bond lengths are moderate, being 0.021 Å or less. As shown in Figure 1, the K^+ ion interacts not only with the oxygen atoms in the crown ether but also with the carbonyl oxygens. A similar interaction (K···O = 2.944(6) Å) was found by Fischer and co-workers in $[K(18\text{-crown-6})]^+[(Ph_2PCH_2CH_2C_5H_4)W(CO)_3]^-$.[48] Both W−$C_{CO}$ bonds of $[CpW(CO)_2(IMes)]^-$ are slightly nonlinear, with W−C−O angles of 171.3(2) and 174.5(2)°. Morris and co-workers found an Os−C−O angle of 174(2)° in $[OsH_3(CO)(P^iPr_3)_2]^-[K(18\text{-crown-6})]^+$.[41] The M−C−O bonding geometry for both of these systems could be affected by K^+−carbonyl interactions in the solid state whose persistence in solution is likely to be solvent-dependent.

Synthesis of $[CpW(CO)_2(IMes)(MeCN)]^+X^-$ ($X^- = PF_6^-$, $B(C_6F_5)_4^-$). Hydride transfer from transition metal hydrides to Ph_3C^+ has been studied extensively. We have reported that hydride transfers from metal hydrides to Ph_3C^+ have rate constants spanning 6 orders of magnitude.[49] Hydride abstraction from an 18-electron metal hydride is typically followed by binding of a solvent molecule, counterion, or other ligand to the coordinatively and electronically unsaturated 16-electron metal cation.[50] Hydride transfer from $CpW(CO)_2(IMes)H$ to $Ph_3C^+PF_6^-$ in MeCN leads to the isolation of $[CpW(CO)_2(IMes)(MeCN)]^+PF_6^-$ as a red crystalline solid in 84% yield (eq 2).

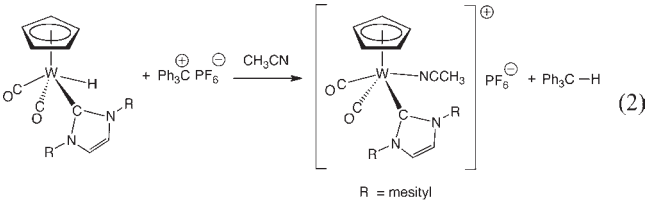

(2)

To examine ion-pairing effects in low-polarity media and to facilitate the measurement of ligand substitution equilibria at the $[CpW(CO)_2(IMes)(L)]^+$ fragment in THF in particular,[45] we developed a method to prepare $[CpW(CO)_2(IMes)(MeCN)]^+B(C_6F_5)_4^-$. The reaction of $CpW(CO)_2(IMes)H$ with $Ph_3C^+B(C_6F_5)_4^-$ in MeCN proceeds similarly to that of the hydride with $Ph_3C^+PF_6^-$, but in this case it affords a red oil containing Ph_3CH and traces of any excess reagent ($CpW(CO)_2(IMes)H$ or $Ph_3C^+B(C_6F_5)_4^-$). An alternate preparation of $[CpW(CO)_2(IMes)(MeCN)]^+B(C_6F_5)_4^-$ from crystalline $[CpW(CO)_2(IMes)]^+B(C_6F_5)_4^-$ is shown in eq 3.

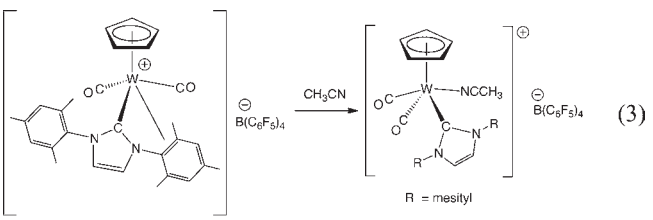

(3)

dx.doi.org/10.1021/ja202754e |J. Am. Chem. Soc. 2011, 133, 14593–14603

Table 1. IR Data (cm^{-1}) for $CpW(CO)_2(IMes)$ Complexes in Different Solvents

		MeCN		THF		*o*-difluorobenzene	
entry	complex	$\nu_{CO,sym}$	$\nu_{CO,asym}$	$\nu_{CO,sym}$	$\nu_{CO,asym}$	$\nu_{CO,sym}$	$\nu_{CO,asym}$
1	$[CpW(CO)_2(IMes)]^+B(C_6F_5)_4^-$					1981	1896
2	$[CpW(CO)_2(IMes)(THF)]^+B(C_6F_5)_4^-$			1965	1863	1971	1869
3	$[CpW(CO)_2(IMes)(MeCN)]^+B(C_6F_5)_4^-$	1968	1872	1969	1878	1969	1878
4	$[CpW(CO)_2(IMes)(MeCN)]^+PF_6^-$	1969	1872	1962	1872	1971	1882
5	$CpW(CO)_2(IMes)^\bullet$	1870	1766	1879	1781	1875	1771
6	$[CpW(CO)_2(IMes)]^-[K(18\text{-crown-}6)]^+$	1743	1662	1765	1664	1740	1657

We previously reported that hydride transfer from $CpW(CO)_2(IMes)H$ to $Ph_3C^+B(C_6F_5)_4^-$ in toluene gives $[CpW(CO)_2(IMes)]^+B(C_6F_5)_4^-$, with structural data showing an η^2-C=C bond between the tungsten and a C=C on one of the IMes mesityl substituents.[47,51] This weak W−arene interaction is readily displaced by alcohols, ketones, or other ligands,[47,51] or by MeCN (eq 3), in this case producing $[CpW(CO)_2(IMes)(MeCN)]^+B(C_6F_5)_4^-$. While still an oil, material prepared in this way is pure by ^1H NMR spectroscopy.

NMR and IR Spectroscopic Characterization of $[CpW(CO)_2(IMes)(S)]^+$ (S = MeCN, THF). The NMR spectroscopic properties of $[CpW(CO)_2(IMes)(MeCN)]^+PF_6^-$ are very similar to those of the recently reported molybdenum analogue *cis*-$[CpMo(CO)_2(IMes)(MeCN)]^+BF_4^-$.[52] At 20 °C in CD_3CN, two sharp signals for the carbonyls are observed in the $^{13}C\{^1H\}$ NMR spectrum, at δ 243.2 and 239.4. The inequivalence of the carbonyls indicates that they are positioned *cis* to each other and that stereoinversion at W is very slow on the NMR time scale. In the ^1H NMR spectrum, two peaks are observed for the mesityl aromatic hydrogens (2 H for each), one singlet for the two vinylic backbone protons, and three singlets (6 H each) in the methyl region (δ 2.5−2.0). A peak at δ 1.95 (3 H) indicates that 1 equiv of free MeCN is formed by exchange of bound MeCN with free CD_3CN. This exchange process is slow on the NMR time scale but goes to completion within 1 h at room temperature. This is inferred from the observation of a small peak at δ 2.36 for W-coordinated MeCN when an ^1H NMR spectrum is recorded soon after dissolution of $[CpW(CO)_2(IMes)(MeCN)]^+$ in CD_3CN. When another ^1H NMR spectrum is recorded 1 h later, the peak at δ 2.36 has disappeared, with an increase in intensity for the resonance of free MeCN. The observation of one vinylic, two aromatic, and three methyl resonances for the IMes ligand in this C_1-symmetric complex indicates that rotation about the $W-C_{IMes}$ bond must be fast on the NMR time scale at 20 °C.

The ^1H NMR spectrum of $[CpW(CO)_2(IMes)(MeCN)]^+PF_6^-$ in THF-d_8 shows a qualitatively similar disposition of signals, but with the appearance of a singlet (3 H) at δ 2.46 assigned to $W-NCCH_3$, significantly downfield compared to the signal for free MeCN in THF-d_8 (δ 1.95). A minor peak (<3%) assigned to the Cp resonance of $[CpW(CO)_2(IMes)(THF\text{-}d_8)]^+$ appears at δ 5.35; this peak disappears upon addition of 2 equiv of MeCN, suggesting that the equilibrium for displacement of THF by MeCN at the cationic tungsten center is highly favorable.[45] Further addition of 13 equiv of MeCN to this THF-d_8 solution has essentially no effect on the positions of the IMes resonances or the $W-NCCH_3$ resonance.

The crystal structure of $[CpW(CO)_2(IMes)]^+B(C_6F_5)_4^-$ showed an η^2 interaction between one of the mesityl rings and the tungsten center (eq 3).[47,51] The solution IR spectrum of this species in *o*-difluorobenzene shows a single dicarbonyl pattern (ν_{CO} = 1981, 1896 cm^{-1}). It is unknown if the W−(C=C) interaction persists in *o*-difluorobenzene. Addition of a small amount of THF cleanly converts this complex to a distinctly new species (ν_{CO} = 1971, 1869 cm^{-1}), assigned to $[CpW(CO)_2(IMes)(THF)]^+B(C_6F_5)_4^-$.

The ^1H NMR spectrum of $[CpW(CO)_2(IMes)(THF\text{-}d_8)]^+B(C_6F_5)_4^-$ in THF-d_8 at 20 °C shows a Cp resonance at δ 5.33 (line width = 2.4 Hz), with significantly broadened IMes resonances (50−200 Hz with overlap). The broadness of the IMes resonances is due to a slower rotation about the $W-C_{IMes}$ bond in the THF-coordinated complex compared to the MeCN-coordinated complex, placing the exchange rate for this rotation in the intermediate regime for $[CpW(CO)_2(IMes)(THF\text{-}d_8)]^+B(C_6F_5)_4^-$. It is likely that the increased steric bulk of THF versus MeCN increases the barrier for carbene rotation in the THF-coordinated complex. The rotation about the $W-C_{IMes}$ bond is fully frozen out at −60 °C, and six nonequivalent IMes methyl signals are observed in the ^1H NMR spectrum.

The ^1H chemical shifts of $[CpW(CO)_2(IMes)(MeCN)]^+B(C_6F_5)_4^-$ in THF-d_8 differ from those of $[CpW(CO)_2(IMes)(MeCN)]^+PF_6^-$ by 0.07 ppm or less, with these small differences likely caused by ion-pairing effects.[53] As with the PF_6^- salt, a small peak (<3%) assigned to $[CpW(CO)_2(IMes)(THF\text{-}d_8)]^+B(C_6F_5)_4^-$ can be detected.

IR spectroscopic data of the carbonyl bands of these complexes in MeCN, THF, and *o*-difluorobenzene solution are given in Table 1. Varying the counteranion of $[CpW(CO)_2(IMes)(MeCN)]^+$ (Table 1, entries 3 and 4; $B(C_6F_5)_4^-$ vs PF_6^-) has no effect on the spectra in MeCN (ε = 36) but has a notable effect with less polar *o*-difluorobenzene (ε = 13.8) or THF (ε = 7.58) as solvent. This indicates that ion-pairing is more prevalent in solvents with lower dielectric constant,[54] an important consideration given our interest in establishing equilibrium constants for the displacement MeCN with H_2, since this displacement cannot be observed with MeCN as solvent.[45]

Synthesis of $CpW(CO)_2(IMes)^\bullet$. Electrochemical oxidation of $[CpW(CO)_2(IMes)]^-[K(18\text{-crown-}6)]^+$ in MeCN (0.2 M $^nBu_4N^+PF_6^-$) is fully reversible at all scan rates, having $E_{1/2}$ = −1.65 V vs $Cp_2Fe^{+/0}$ (Figure 2). This contrasts with the behavior of the parent anion $[CpW(CO)_3]^-$, for which an irreversible oxidation wave is observed,[55] due to the rapid dimerization of the resulting $CpW(CO)_3^\bullet$ radicals. The apparent persistence of the radical $CpW(CO)_2(IMes)^\bullet$ prompted our efforts to isolate it. Combining equimolar solutions of $[CpW(CO)_2(IMes)]^-[K(18\text{-crown-}6)]^+$ and $[CpW(CO)_2(IMes)(MeCN)]^+PF_6^-$

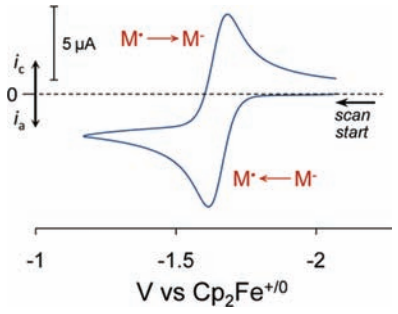

Figure 2. Cyclic voltammogram showing the oxidation of $[CpW(CO)_2(IMes)]^-[K(18\text{-crown-6})]^+$ (2 mM) in MeCN (0.2 M $^nBu_4N^+PF_6^-$) at 0.1 V s^{-1}. M = $CpW(CO)_2(IMes)$.

results in complete conversion to a single new species through a comproportionation reaction (eq 4).

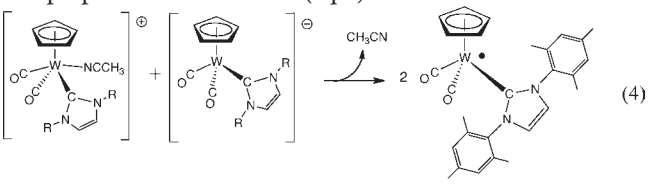

(4)

Figure 3 shows the IR spectra of THF solutions of $[CpW(CO)_2(IMes)(MeCN)]^+$ and $[CpW(CO)_2(IMes)]^-$, along with a spectrum of the resultant mixture, featuring a new pair of IR bands in the CO stretching region and the disappearance of bands

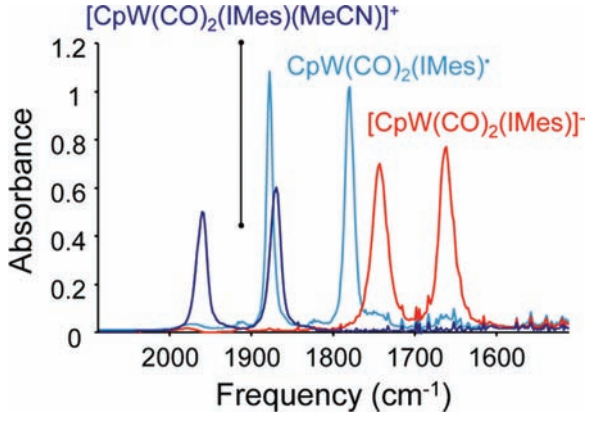

Figure 3. THF solution IR absorption spectra showing the CO stretching region of $[CpW(CO)_2(IMes)]^-[K(18\text{-crown-6})]^+$ (red), $[CpW(CO)_2(IMes)(MeCN)]^+PF_6^-$ (dark blue), and $CpW(CO)_2(IMes)^•$ (light blue) prepared by combining equimolar solutions of $[CpW(CO)_2(IMes)]^-$ and $[CpW(CO)_2(IMes)(MeCN)]^+$.

corresponding to starting materials. With THF as solvent, the $K^+PF_6^-$ byproduct precipitates, simplifying the purification of the new species. $CpW(CO)_2(IMes)^•$ may also be prepared by reduction of $[CpW(CO)_2(IMes)(MeCN)]^+PF_6^-$ with cobaltocene in THF (eq 5); $Cp_2Co^+PF_6^-$ precipitates during the reaction.

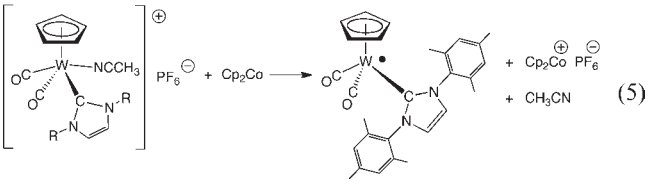

(5)

Solid-State Structure of $CpW(CO)_2(IMes)^•$. The crystal structure of $CpW(CO)_2(IMes)^•$ was determined by single-crystal XRD, showing a three-legged piano-stool configuration (Figure 4). The asymmetric unit contains two symmetry-inequivalent but geometrically similar formula units packed head-to-tail, with the carbonyl O atoms being closest to the IMes vinyl H atoms of the adjacent unit. The shortest W···W distance is 8.414 Å, confirming that the formula unit is monomeric. As indicated by the small difference in $C_{carbene}-W-C_{CO}$ angles, the CO ligands are somewhat asymmetrically disposed with respect to the $C_{carbene}-W-Cp_{centroid}$ plane, although not unequivocally *cis* and *trans* with respect to the carbene ligand. In contrast, the $CpCr(CO)_2(PPh_3)^•$ radical is nearly C_s-symmetric.[1,18] In the structure of $CpW(CO)_2(IMes)^•$, the $N-C_{carbene}-N$ plane is oblique with respect to the $C_{carbene}-W-Cp_{centroid}$ plane, with one mesityl group oriented toward the Cp ring and the other in close proximity to the C(27)−O(1) ligand. The other CO ligand occupies the pocket between the two mesityl rings. These structural features are well-reproduced by gas-phase DFT calculations (see below), suggesting that the asymmetry arises from mutual accommodation of the bulky IMes ligand and the CO ligands, rather than crystal packing effects.

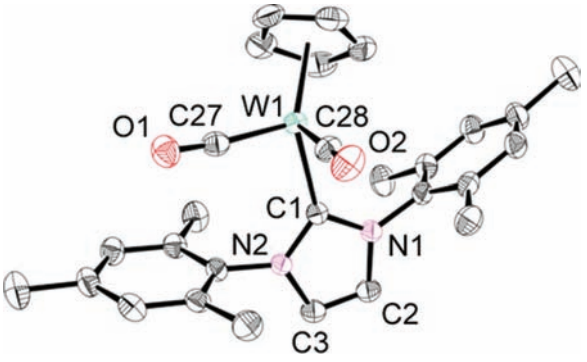

Figure 4. Molecular structure of $CpW(CO)_2(IMes)^•$ (one of two crystallographically inequivalent molecules) with the atom labeling scheme. Thermal ellipsoids are scaled to 30% probability. Selected bond lengths (Å) and angles (°) (one of two symmetry-inequivalent molecules): W(1)−C(1) 2.164(4), W(1)−C(27) 1.935(5), W(1)−C(28) 1.930(4), C(27)−O(1) 1.176(5), C(28)−O(2) 1.168(5), $Cp_{centroid}-W(1)$ 2.033(2); C(27)−W(1)−C(28) 79.47(18), C(1)−W(1)−C(27) 98.75(16), C(1)−W(1)−C(28) 89.60(15), W(1)−C(27)−O(1) 173.3(4), W(1)−C(28)−O(2) 176.3(4).

Structural metrics of both independent formula units are sufficiently different from those of the known structure of $CpW(CO)_2(IMes)H$[47] to rule out the possibility that the crystal sample was actually $CpW(CO)_2(IMes)H$ and not the radical $CpW(CO)_2(IMes)^•$. Comparison of both $CpW(CO)_2(IMes)^•$ formula units with the hydride shows no overlap of the 2σ confidence intervals for the $W-C_{carbene}$ distance, the $C_{CO}-W-C_{CO}$ angle, or the $C_{CO}-W-C_{carbene}$ angles. This is because the hydride structure features CO ligands that are decidedly *cis* and *trans* with respect to the carbene ligand, whereas the radical does not.

EPR Spectra of $CpW(CO)_2(IMes)^•$. The low-spin 17-electron W(I) d^5 radical $CpW(CO)_2(IMes)^•$ is EPR active;[56] its EPR spectrum at room temperature in toluene solution (ca. 1 mM) features a broad resonance at $g_{iso} = 2.15$ with a line width (W) of

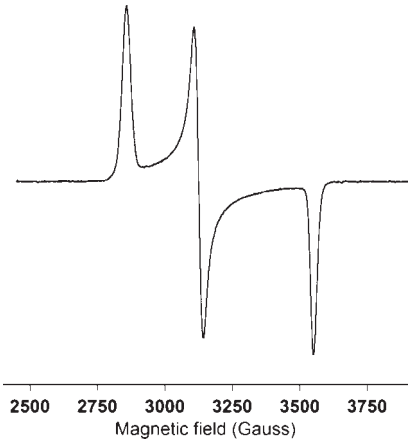

Figure 5. X-band (9.466 GHz) EPR spectrum of $CpW(CO)_2(IMes)^{\bullet}$ in frozen toluene solution at 80 K.

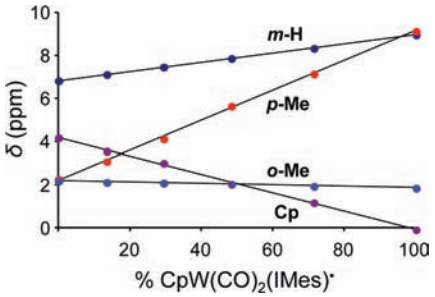

Figure 6. Cp and IMes ^{1}H NMR chemical shifts for mixtures of rapidly exchanging $CpW(CO)_2(IMes)^{\bullet}$ and $[CpW(CO)_2(IMes)]^-[K(18\text{-crown-}6)]^+$ as a function of solution composition. Spectra were collected in THF-d_8 at 20 °C. *o*-Me, *m*-H, and *p*-Me refer to IMes aryl substituents. The vinyl resonance, which evolves from δ 6.62 (s, 0.63 Hz) to δ 23.17 (br, 300 Hz) with increasing fractional radical content, has been omitted for clarity.

190(10) G. Cooling the solution to 200 K results in a modest reduction of the line width to 160(10) G, and sharper spectra are obtained in frozen toluene solution. The spectrum recorded at 80 K (Figure 5) displays rhombic symmetry as expected for a C_1- or C_s-symmetric radical; the parameters obtained from spectral simulation are $g_1 = 2.367$ ($W_1 = 32(3)$ G), $g_2 = 2.164$ ($W_2 = 28(3)$ G), and $g_3 = 1.904$ ($W_3 = 24(3)$ G; see Figures S1−S3, Supporting Information). Although $CpW(CO)_2(IMes)^{\bullet}$ may assume average C_s symmetry in fluid solution by rotation about the W−$C_{carbene}$ bond, it is likely that it assumes C_1 symmetry in the frozen solution, as the observed and calculated ground-state symmetry of $CpW(CO)_2(IMes)^{\bullet}$ is C_1. Despite the significant reduction in line width upon cooling to 80 K, hyperfine coupling to tungsten (^{183}W, $I = 1/2$, 14.4% natural abundance) was still not discernible in any of the three peaks, and further cooling of the sample to 7 K did not result in any additional sharpening of the signals. However, the *g*-anisotropy leaves no doubt that the radical is mainly tungsten-based. DFT calculations (vide infra) indicate a spin density at tungsten of ca. 63%; expected hyperfine coupling constants to tungsten of ca. 30−50 G are low enough that the tungsten satellites are simply not resolved.

Connelly and co-workers characterized the octahedral W(I) radical $Tp^*W(CO)_2(\eta^2\text{-MeC}{\equiv}\text{CMe})^{\bullet}$ (Tp^* = hydridotris(3,5-dimethylpyrazolyl)borate),[21] observing a 77 K EPR spectrum like that of $CpW(CO)_2(IMes)^{\bullet}$ (Figure 5), albeit with less severe anisotropy ($g_1 = 2.102$, $g_2 = 2.015$, $g_3 = 1.955$), and with small enough line widths to reveal hyperfine coupling to ^{183}W (37−53 G). Because of their generally high (dimerization) reactivity, neutral W(I) piano-stool radicals have not been characterized previously by EPR spectroscopy. The EPR spectrum of the closely related molybdenum derivative $CpMo(CO)_2(IMes)^{\bullet}$ was recorded by Tumanskii and co-workers,[34] although it was generated in situ in the EPR cavity and not isolated. It also has lower anisotropy ($g_1 = 2.129$, $g_2 = 2.061$, $g_3 = 1.993$) than the W derivative in frozen toluene solution, and the spectrum at 260 K was sharp enough that coupling to $^{95/97}$Mo ($a_{Mo} = 17$ G) was observed. Very thorough EPR and theoretical studies of the Cr(I) piano-stools $CpCr(CO)_3^{\bullet}$, $Cp^*Cr(CO)_3^{\bullet}$, $CpCr(CO)_2(PPh_3)^{\bullet}$, and $Cp^*Cr(CO)_2(PMe_3)^{\bullet}$ have been reported.[57] In all of these complexes, as is the case for $CpW(CO)_2(IMes)^{\bullet}$, one principal *g* value is lower than that of the free electron (g_e = 2.0023), and the remaining two are higher.

NMR Spectral Features, NMR Peak Assignments, and Degenerate Electron Transfer Exchange between $CpW(CO)_2(IMes)^{\bullet}$ and $[CpW(CO)_2(IMes)]^-[K(18\text{-crown-}6)]^+$. The ^{1}H NMR spectra of $CpW(CO)_2(IMes)^{\bullet}$ show chemical shifts spanning 24 ppm, with half-height peak widths ranging from 35 to over 500 Hz. As with the isostructural tungsten anion $[CpW(CO)_2(IMes)]^-[K(18\text{-crown-}6)]^+$, one signal each is observed for the *o*-Me, *m*-H, *p*-Me, and vinyl protons. Solutions containing $CpW(CO)_2(IMes)^{\bullet}$ and $[CpW(CO)_2(IMes)]^-[K(18\text{-crown-}6)]^+$ in THF-d_8 exhibit rapid degenerate chemical exchange at room temperature, with ^{1}H peak positions evolving linearly with solution composition for a series of radical-anion mixtures (Figure 6). Peak assignments for the radical were made using these spectra by tracing the chemical shifts of signals assigned for the anion as the fractional radical concentration was increased.[58] The rate constant at 20 °C for degenerate electron transfer between the anion and isostructural radical is $1.2(7) \times 10^6$ M^{-1} s^{-1} (error at the 2σ confidence level), as determined using full line shape analysis of the ^{1}H NMR spectra. For comparison, a second-order rate constant of 8.6×10^6 M^{-1} s^{-1} was determined at 30 °C for degenerate electron exchange between the 17-electron radical $Tp^*(CO)_3Mo^{\bullet}$ and the anion $[Tp^*(CO)_3Mo]^-$ in THF.[59] Self-exchange rates for interconversion of Fe(II) and Fe(III) homologues of the form $[Cp^*Fe(dppe)(C{\equiv}C\text{-arene})]^{n+}$ ($n = 0, 1$) determined in CD_2Cl_2 at 20 °C ranged from 1.33×10^8 to 2.58×10^8 M^{-1} s^{-1}.[58]

Stability of $CpW(CO)_2(IMes)^{\bullet}$ with Respect to Dimerization. The NMR, EPR, electrochemical, and single-crystal XRD results presented above indicate that $CpW(CO)_2(IMes)^{\bullet}$ exists as an odd-electron monomeric complex both in solution and in the solid state. However, none of these results demonstrate that the dimer is inaccessible. We have undertaken a series of temperature- and concentration-dependent NMR studies and an IR concentration study to establish whether dimerization can occur.

In a series of experiments examining dilution effects at 25 °C on $CpW(CO)_2(IMes)^{\bullet}$ in toluene-d_8, ^{1}H chemical shifts for all resonances were found to be independent of concentration across a range from the saturation limit (8.7 mM) approaching the detection limit (0.68 mM), with no evidence across these spectra for diamagnetic $[CpW(CO)_2(IMes)]_2$ either in

exchange or as a spectroscopically distinct species. We found that the solubility of $CpW(CO)_2(IMes)^\bullet$ is higher in fluorobenzene than in toluene, so we collected a series of IR spectra in fluorobenzene with concentrations of $CpW(CO)_2(IMes)^\bullet$ ranging from the saturation limit (0.3 M) through three 1:10 dilutions to 0.3 mM. Increasing the concentration does not appear to produce any new CO stretches or any change in the shape of the CO bands of the radical, suggesting that no dimeric material is present, even in saturated fluorobenzene solution.

Wayland and co-workers presented an expression describing how δ_{obs} varies with temperature for a diamagnetic dimer in rapid equilibrium exchange with paramagnetic monomer units.[60] Use of this expression with ^{1}H NMR shift data of $CpW(CO)_2(IMes)^\bullet$ collected in toluene-d_8 over the range from −60 to 20 °C produces dimer concentration estimates approaching zero.

Reaction of $CpW(CO)_2(IMes)^\bullet$ with H_2. Hoff and co-workers found that $Cp^*Cr(CO)_3^\bullet$ reacts with H_2 to produce the chromium hydride $Cp^*Cr(CO)_3H$.[61] They found that the reaction exhibits third-order kinetics, with a substantial negative entropy of activation ($\Delta S^\ddagger = -47 \pm 4$ cal mol^{-1} K^{-1}), suggesting a termolecular transition state. Wayland and co-workers have reported extensive kinetic and thermochemical studies of similar reactions of Rh(II) complexes with bulky porphyrin ligands that react with H_2[62] or methane;[63] their reactions also exhibit third-order kinetics. We have found that $CpW(CO)_2(IMes)^\bullet$ reacts with H_2 over a period of several days in toluene-d_8 under 4 atm H_2 to generate the neutral hydride $CpW(CO)_2(IMes)H$.

$$2\,Cp(CO)_2(IMes)W^\bullet + H_2 \rightarrow 2\,Cp(CO)_2(IMes)W{-}H \qquad (6)$$

The solution $\Delta G°$ value for W−H bond homolysis (59.3(3) kcal mol^{-1})[45] in MeCN is sufficiently high that the reaction shown in eq 6 is expected to proceed in MeCN as it does under the present conditions in toluene-d_8 (see the Supporting Information).

DFT Calculations of Tungsten Hydrides, Tungsten Radicals, and W−W Bonded Complexes. DFT calculations were carried out on the tungsten hydride $CpW(CO)_2(IMes)H$ and the corresponding radical $CpW(CO)_2(IMes)^\bullet$. These calculations were validated through comparison with experimentally determined geometries and bond energies, and they served to elucidate the electronic structure of the radical. To evaluate the importance of sterics vs electronics on stabilization of $CpW(CO)_2(IMes)^\bullet$ and to investigate bonding in putative W−W bonded dimers, calculations were also carried out on related radical complexes $CpW(CO)_2(IH)^\bullet$ and $CpW(CO)_2(IMe)^\bullet$ having less sterically demanding NHC ligands IMe (1,3-dimethylimidazol-2-ylidene, with *N*-methyl groups) and IH (1,3-dihydroimidazol-2-ylidene, having *N*-H substituents), and on the corresponding dimers. Results of these calculations support the hypothesis that the stability of $CpW(CO)_2(IMes)^\bullet$ is largely due to the steric bulk of the IMes ligand rather than spin delocalization.

Calculated geometries for $CpW(CO)_2(IMes)^\bullet$ and $CpW(CO)_2(IMes)H$ are in good agreement with those determined by XRD, with calculated bond lengths about 1−3% longer and bond angles within 1−3° (see Figure S5 and Table S2, Supporting Information).[47] The optimized geometries were used to calculate room-temperature enthalpies of formation for $CpW(CO)_2(IMes)^\bullet$ and $CpW(CO)_2(IMes)H$ (Table S5, Supporting Information), giving a W−H homolytic bond dissociation energy (BDE) of 63 kcal mol^{-1} (Table 2). The experimentally determined W−H bond dissociation *free* energy (59.3 kcal mol^{-1})[45] corresponds[45,64] to a BDE of 65 kcal mol^{-1}, in agreement with the computed value within 2 kcal mol^{-1}.

Table 2. Computed Bond Dissociation Energies of Tungsten Hydrides (W−H) and Tungsten Dimers (W−W)

entry	complex	calcd BDE (kcal mol^{-1})
	Tungsten Hydrides	
1	$CpW(CO)_2(IMes)H$	62.99
2	$CpW(CO)_2(IMe)H$	64.05
3	$CpW(CO)_2(IH)H$	66.96
	Tungsten Dimers	
4	$[CpW(CO)_2(IMe)]_2$	5.95
5	$[CpW(CO)_2(IH)]_2$	17.70

Table 3. Spin Density Distributions by Ligand for $CpW(CO)_2(NHC)^\bullet$ Radicals (NHC = IMes, IMe, IH)

		spin density (%)				
entry	complex	W	Cp	CO	CO	NHC
1	$CpW(CO)_2(IMes)^\bullet$	63	7	16	2	12
2	$CpW(CO)_2(IMe)^\bullet$	68	8	8	10	5
3	$CpW(CO)_2(IH)^\bullet$	74	7	8	8	3

The calculated unpaired spin distribution of $CpW(CO)_2(IMes)^\bullet$ has 63% of the spin density at W, with much of the remainder delocalized asymmetrically over one of the carbonyl ligands (16%) and the NHC ligand (12%), suggesting that spin delocalization into the NHC ligand does not contribute uniquely to the stability of the radical (Table 3; spin densities at the atom level are given in Table S6, Supporting Information). Notably, the calculated structures of $CpW(CO)_2(IMe)^\bullet$ and $CpW(CO)_2(IH)^\bullet$ approach C_s symmetry (see Figure S6, Supporting Information), and the spin density is distributed much more evenly across the two carbonyl ligands than in the C_1-symmetric $CpW(CO)_2(IMes)^\bullet$.

While experiments and calculations show that $CpW(CO)_2(IMes)^\bullet$ does not dimerize, calculations suggest that $CpW(CO)_2(IMe)^\bullet$ and $CpW(CO)_2(IH)^\bullet$ form weakly bonded dimers (Figure 7), in accordance with the experimentally observed dimerization of the parent $CpW(CO)_3^\bullet$. Although no symmetry contraints were used in the optimization procedure, we found that $[CpW(CO)_2(IH)]_2$ and $[CpW(CO)_2(IMe)]_2$ minimize to essentially C_i and C_2 symmetry, respectively. The parent $[CpW(CO)_3]_2$ has C_{2h} symmetry; it is likely that both $[CpW(CO)_2(NHC)]_2$ species would adopt averaged C_{2h} symmetry in solution as well.

The calculated W−W bond length in $[CpW(CO)_2(IH)]_2$ is 3.324 Å (see Table S4, Supporting Information, for more geometrical parameters), and the dimer is calculated to be 18 kcal mol^{-1} more stable than the monomeric fragments. The IH carbene is oriented somewhat asymmetrically in the dimer, with an N−H unit pointing to a carbonyl, possibly due to intramolecular H-bonding, judging from the short separation of 2.261 Å between H(16) and O(5). This interaction may also be responsible for the significant bending of the angle W(1)−C(4)−O(5) down to 169°. $[CpW(CO)_2(IMe)]_2$ is significantly less stabilized, being only 6 kcal mol^{-1} more stable than its monomeric fragments. It has a calculated W−W bond length of 3.430 Å, which is 0.106 Å longer than that in $[CpW(CO)_2(IH)]_2$. Furthermore, there are signs of severe steric

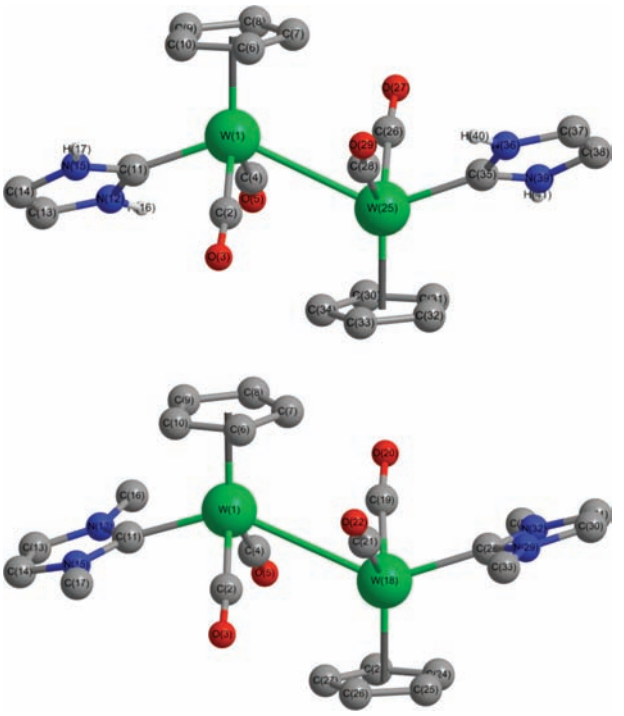

Figure 7. Optimized calculated structures of $[CpW(CO)_2(IH)]_2$ (top) and $[CpW(CO)_2(IMe)]_2$ (bottom).

crowding within this dimer. To minimize repulsive interactions between the *N*-methyl substituents and the carbonyl carbons, the angle W−W′−$C_{carbene}$ increases to 138° (133° for the IH analogue), and the average $C_{carbene}$−W−C_{CO} angle increases to 84.7° (80.5° for the IH analogue). Considering the only very modest stabilization of $[CpW(CO)_2(IMe)]_2$, it can be expected to be in equilibrium with observable amounts of the monomeric radical $CpW(CO)_2(IMe)^\bullet$ in solution; experimental studies to test this possibility are currently underway.

CONCLUSIONS

The 17-electron radical $CpW(CO)_2(IMes)^\bullet$ is an unusual example of a third-row metal radical that has been isolated and characterized by NMR, IR, and EPR spectroscopy and single-crystal XRD. Our data indicate that IMes is a very strong donor, even compared to phosphines, a topic that is explored further in our studies of W−H thermochemistry of $CpW(CO)_2(IMes)H$ and species related to it by oxidation or homolytic or heterolytic W−H scission.[45] Comparison of structural and spectroscopic data of $[CpW(CO)_2(IMes)]^-[K(18\text{-crown-6})]^+$, $CpW(CO)_2(IMes)^\bullet$, $CpW(CO)_2(IMes)H$,[47] and $[CpW(CO)_2(IMes)]^+B(C_6F_5)_4^-$ [47,51] reveals that, consistently across this series, as the W−C_{IMes} bond distance increases, both oxidation potentials and CO stretching IR frequencies increase. EPR and computational studies indicate that the unpaired spin of $CpW(CO)_2(IMes)^\bullet$ resides primarily at W. This species is monomeric both in the solid state and in solution under all conditions studied; its observed stability permits consideration of catalytic cycles in which it participates as an intermediate, in contrast with similar Group 6 radical species that readily dimerize. This stability vs dimerization has been examined computationally and appears to be primarily attributable to sterics of the bulky mesityl groups of $CpW(CO)_2(IMes)^\bullet$. Most of the known paramagnetic complexes with NHC ligands are first-row metal complexes. The studies reported here on $CpW(CO)_2(IMes)^\bullet$ show that paramagnetic third-row metal complexes with NHC ligands can be stable if sufficient steric bulk on a ligand is present to prevent dimerization or atom abstraction reactions.

EXPERIMENTAL SECTION

Methods and Materials. All manipulations were carried out under N_2 using standard vacuum line, Schlenk, and inert-atmosphere glovebox techniques. Filtrations were carried out in the glovebox either with medium-porosity glass fritted funnels or 0.45-μm Teflon syringe filters. $CpW(CO)_2(IMes)H$ was prepared as previously described.[47] THF (Alfa-Aesar, anhydrous, nonstabilized), toluene (EMD, spectrophotometric grade), and hexanes (Fisher GC Resolv) were purified by passage through neutral alumina using an Innovative Technology, Inc. PureSolv solvent purification system. Fluorobenzene (EMD) and *o*-difluorobenzene (Aldrich) were stirred for 1 week over P_2O_5 and then vacuum distilled through a glass wool plug. THF-d_8 and toluene-d_8 (Cambridge Isotope Laboratories, 99.5% D or greater) were vacuum distilled after being stirred for several days over NaK. Cobaltocene (Strem) was used as received. Triphenylmethylsilane (used as an internal standard for NMR integration) was prepared by reacting triphenylchlorosilane in diethyl ether (Aldrich) with 1.1 equiv of methyllithium (1.0 M in diethyl ether, Aldrich) at −78 °C, warming, filtering, and vacuum drying. The product was purified by sublimation. $^nBu_4N^+PF_6^-$ (Aldrich) was recrystallized from methanol−diethyl ether and dried *in vacuo* at 150 °C for 16 h. Ferrocene (Aldrich), decamethylferrocene (Aldrich), and $Cp_2Co^+PF_6^-$ (Cole-Parmer) were used as received.

Instrumentation. Electrochemical measurements were performed using a CH Instruments 660C potentiostat equipped with a standard three-electrode cell, which was assembled and used within the glovebox. The working electrode (1-mm dia. polyether ether ketone-encased glassy carbon, Cypress Systems EE040) was polished using alumina (BAS CF-1050, dried at 150 °C under vacuum) suspended in MeCN and then rinsed with neat MeCN. A glassy carbon rod (Structure Probe, Inc.) was used as the counterelectrode, and a silver wire suspended in a solution of $^nBu_4N^+PF_6^-$ (0.2 mM) in MeCN and separated from the analyte solution by a Vycor frit (CH Instruments 112) was used a pseudoreference electrode. All potentials are reported vs the $Cp_2Fe^{+/0}$ couple, and all reported potentials were determined vs a redox couple of a known internal reference compound: $Cp_2Fe^{+/0}$, $(C_5Me_5)_2Fe^{+/0}$ ($E°$ = −0.50 V vs $Cp_2Fe^{+/0}$), or $Cp_2Co^{+/0}$ ($E°$ = −1.33 V vs $Cp_2Fe^{+/0}$). NMR spectroscopic experiments were carried out using a Varian Unity INOVA 500 MHz spectrometer, with the probe temperature regulated to 20 °C unless otherwise noted. Chemical shifts were referenced to the residual solvent peak. EPR spectra were recorded at or below 1 mM (no concentration dependence on shape of signal observed) in liquid or frozen toluene solutions, using a Bruker Elexsys X-band EPR spectrometer equipped with a helium-cooled cryostat. Simulation of the spectra was done with WinEPR SimFonia version 1.26, and *g* values were derived from the field/frequency ratios. More details can be found in the Supporting Information. Solution IR spectra were recorded using a Nicolet Magna-IR 860 FTIR spectrometer with sealed liquid CaF_2 cells. Elemental analyses were performed by Galbraith Laboratories and Atlantic Microlab. Digital simulation of NMR line shapes was carried out using gNMR Version 5.0.6.0.[65] Details of the X-ray diffractometry experiment and crystallographic information (.cif) files are provided in the Supporting Information.

$[CpW(CO)_2(IMes)]^-[K(18\text{-crown-6})]^+$. A solution of $CpW(CO)_2(IMes)H$ (319 mg, 0.523 mmol) in THF (10 mL) was added to solid KH (217 mg, 5.41 mmol). To the resulting suspension was

added a solution of 18-crown-6 (154 mg, 0.583 mmol) in THF (2 mL) dropwise over 5 min, with immediate gas evolution accompanied by a yellow-to-orange color change. This mixture was stirred for 2 h. The resulting suspension was filtered, and solvent was removed from the filtrate under vacuum until the onset of precipitation, at which point the solution was warmed to redissolve the precipitate. This deep orange solution was layered with diethyl ether (15 mL) and allowed to stand for 2 days, giving bright orange needles with a pale yellow supernatant which was decanted off. The solids were rinsed with diethyl ether (3 × 2 mL) and then hexanes (2 × 2 mL) and dried under vacuum, giving $[CpW(CO)_2(IMes)]^-[K(18\text{-crown-}6)]^+$ as microcrystalline orange needles (292 mg, 0.295 mmol, 56% yield) containing 0.5 equiv of THF, as determined by ^1H NMR. The supernatant was allowed to stand for several days, with slow formation of orange needles followed by their slow disappearance simultaneous with formation of large red blocks that were used for single-crystal XRD. Large orange needles were also isolated by slow diffusion of hexanes into THF solutions of $[CpW(CO)_2(IMes)]^-[K(18\text{-crown-}6)]^+$, but these samples did not diffract well enough for structural determination. Anal. Calcd for $C_{40}H_{53}N_2O_8WK$: C, 52.67; H, 5.86; N, 3.07. Found: C, 51.63; H, 5.76; N, 3.02. Solution IR data (MeCN, THF, *o*-difluorobenzene) are given in Table 1. ^1H NMR (25 °C, THF-d_8): δ 6.85 (IMes *m*-H, 4 H, br, full width at half-maximum (fwhm) = 5.9 Hz), 6.62 (IMes vinyl, 2 H, s, 0.63 Hz), 4.20 (Cp, 5 H, s, 0.68 Hz), 3.56 (18-crown-6 methylene, 24 H, br, 3.7 Hz), 2.26 (IMes *p*-Me, 6 H, br, 6.4 Hz), 2.20 (IMes *o*-Me, 12 H, br, 9.4 Hz). ^1H NMR (CD_3CN): δ 6.91 (IMes vinyl, 2 H, br, 2.9 Hz), 6.87 (IMes *m*-H, 4 H, br, ~50 Hz), 4.06 (Cp, 5 H, br, 6.0 Hz), 3.56 (18-crown-6 methylene, 24 H, s, 0.60 Hz), 2.35 (IMes *p*-Me, 6 H, br, 7.6 Hz), 2.13 (IMes *o*-Me, 12 H, br, 2.6 Hz).

Reductant effects on low-temperature (−60 °C) ^1H NMR line widths of $[CpW(CO)_2(IMes)]^-[K(18\text{-crown-}6)]^+$ were studied by ^1H NMR in THF-d_8 solution. With 1 drop of NaK added, low-temperature line broadening was found to be moderate by comparison with line broadening observed with the same sample before NaK was added. With added NaK, a reduction in temperature (20 → −60 °C) left the vinyl resonance essentially unchanged (0.63 → 0.70 Hz), while the Cp resonance broadened slightly (0.68 → 1.2 Hz), the *o*-Me resonance narrowed (9.4 → 6.3 Hz), and the *m*-H and *p*-Me signals narrowed slightly (5.9 → 5.8 and 6.4 → 5.8 Hz, respectively). The observed sharpening of the *o*-Me signal at reduced temperatures may be due to a temperature dependence in the ion-pairing equilibrium constant. No equilibrium exchange processes in the $[CpW(CO)_2(IMes)]^-$ moiety are evident from these experiments.

$[CpW(CO)_2(IMes)(MeCN)]^+PF_6^-$. A solution of $Ph_3C^+PF_6^-$ (324 mg, 0.834 mmol) in MeCN (10 mL) was added dropwise over 15 min to a solution of $CpW(CO)_2(IMes)H$ (527 mg, 0.864 mmol) in MeCN (125 mL), producing a rapid color change of the solution from yellow to red. This mixture was stirred for 1 h and then filtered. Volatiles were removed under vacuum, and the residue was held under dynamic vacuum overnight. THF (3 mL) was added, causing first dissolution of the oily residue and then precipitation of a red solid. Hexanes (50 mL) were layered onto the deep red suspension, and the mixture was allowed to stand for 4 h, giving a clear orange supernatant that was decanted away. These solids were rinsed with hexanes (3 × 3 mL) and dried under vacuum to give $[CpW(CO)_2(IMes)(MeCN)]^+PF_6^-$ as a microcrystalline red solid (607 mg, 0.703 mmol, 84% yield) having one molecule of crystallization THF per formula unit, as determined by ^1H NMR. Alternatively, this material may be recrystallized by cooling a concentrated *o*-difluorobenzene solution to −45 °C, followed by filtration, rinsing with hexanes, and drying under vacuum. Material isolated in this way shows ^1H NMR and IR spectra identical to those of the material isolated from THF solution, and this material was employed for elemental analysis. Anal. Calcd for $C_{36}H_{36}N_3O_2WPF_8$ (formula includes 1 equiv of crystallization solvent, *o*-difluorobenzene, per W): C, 47.57; H, 3.99; N, 4.62. Found: C, 46.48; H, 3.91; N, 4.74. Solution IR data (MeCN, THF, *o*-difluorobenzene) are given in Table 1. ^1H NMR (CD_3CN): δ 7.45 (IMes vinyl, 2 H, s, fwhm = 0.74 Hz), 7.14 (IMes *m*-H, 2 H, br, 4.1 Hz), 7.08 (IMes *m*-H, 2 H, mult., 4.1 Hz), 5.09 (Cp, 5 H, s, 0.66 Hz), 2.36 (IMes *o*-Me or *p*-Me, 6 H, s, 1.8 Hz), 2.10 (IMes *o*-Me or *p*-Me, 6 H, s, 1.6 Hz), 2.02 (IMes *o*-Me or *p*-Me, 6 H, s, 1.7 Hz), 1.95 (residual MeCN, 3 H, s). ^1H NMR (THF-d_8): δ 7.59 (IMes vinyl, 2 H, s, 1.7 Hz), 7.18 (IMes *m*-H, 2 H, br, 4.8 Hz), 7.08 (IMes *m*-H, 2 H, br, 4.8 Hz), 5.22 (Cp, 5 H, s, 1.7 Hz), 2.47 (CH_3CN, 3 H, s, 1.8 Hz), 2.37 (IMes *o*-Me or *p*-Me, 6 H, s, 1.9 Hz), 2.19 (IMes *o*-Me or *p*-Me, 6 H, s, 2.6 Hz), 2.10 (IMes *o*-Me or *p*-Me, 6 H, s, 2.7 Hz). $^{13}C\{^1H\}$ NMR (125 MHz, 22 °C, CD_3CN): δ 243.2 (W−CO, s, $^1J_{CW}$ = 130 Hz), 239.4 (W−CO, s, $^1J_{CW}$ = 168 Hz), 171.9 (W−CN_2, s, $^1J_{CW}$ = 120 Hz), 141.5 (W−$NCCD_3$, br), 140.9, 137.5, 137.0 (all mesityl quaternary C, s), 130.3, 130.0 (both mesityl CH, s), 127.1 (vinyl, s), 93.9 (Cp, s, $^1J_{CW}$ = 5 Hz), 21.1, 18.7, 18.5 (all mesityl CH_3, s), 5.1 (W−$NCCD_3$, septet, $^1J_{CD}$ = 21 Hz).

$[CpW(CO)_2(IMes)(MeCN)]^+B(C_6F_5)_4^-$. Solid $[CpW(CO)_2(IMes)]^+B(C_6F_5)_4^-$ (15 mg) was dissolved in MeCN (0.02 mL) to afford a deep orange-red solution. Volatiles were removed, giving a red oil that was dissolved in Et_2O (1 mL). Volatiles were again removed, this cycle being repeated five times. Final evacuation afforded a deep red oil containing 1.03 equiv total (bound + free) of MeCN and 0.99 equiv of diethyl ether. Solution IR data (MeCN, THF, *o*-difluorobenzene) are given in Table 1. ^1H NMR (THF-d_8): δ 7.67 (IMes vinyl, 2 H, s, fwhm = 1.6 Hz), 7.17 (IMes *m*-H, 2 H, br, 4.5 Hz), 7.11 (IMes *m*-H, 2 H, br, 4.3 Hz), 5.15 (Cp, 5 H, s, 1.6 Hz), 2.52 (CH_3CN, 3 H, s, 1.7 Hz), 2.38 (IMes *o*-Me or *p*-Me, 6 H, br, 2.7 Hz), 2.16 (IMes *o*-Me or *p*-Me, 6 H, br, 3.4 Hz), 2.09 (IMes *o*-Me or *p*-Me, 6 H, br, 2.4 Hz).

$CpW(CO)_2(IMes)^\bullet$. *Method 1.* A solution of $[CpW(CO)_2(IMes)]^-[K(18\text{-crown-}6)]^+$ (55.2 mg, 57.9 μmol) in THF (4 mL) was added dropwise to a stirred solution of $[CpW(CO)_2(IMes)(MeCN)]^+PF_6^-\cdot$THF (49.6 mg, 57.5 μmol) in THF (6 mL) over 10 min, with rapid red → orange solution color change and formation of a fine precipitate. This mixture was stirred for 90 min, and solvent was removed under vacuum. The residue was extracted with toluene (10 mL, stirred overnight) and filtered, the precipitate being rinsed with toluene (2 × 0.5 mL). The collected red-orange filtrate was concentrated just until a brown precipitate was observed, and then it was placed in a −35 °C freezer overnight, yielding further precipitate. Two additional crops were isolated in this way from the supernatant. Each batch of material was rinsed with hexanes (2 mL), and the combined solids were dried under vacuum, affording iridescent bronze flakes. Yield: 42.3 mg (60%). A single crystal suitable for XRD was isolated by allowing a concentrated solution of $CpW(CO)_2(IMes)^\bullet$ in toluene to stand at −35 °C for several days.

Method 2. A solution of cobaltocene (21.5 mg, 114 μmol) in THF (2 mL) was added dropwise to a stirred solution of $[CpW(CO)_2(IMes)(MeCN)]^+PF_6^-\cdot$THF (101 mg, 117 μmol) in THF (10 mL) over 4 min, with gradual red → orange solution color change and formation of a yellow precipitate. This mixture was stirred for 4 h and then passed through a 0.45-μm poly(tetrafluoroethylene) (PTFE) syringe filter. Solvent was removed under vacuum, and the residue was dissolved in toluene (20 mL) and stirred overnight. This cloudy orange-red liquid was filtered through a 0.45-μm PTFE syringe filter, and the resulting clear solution was concentrated to a final volume of 2 mL, to which was added 15 mL of hexanes. The pale yellow supernatant was decanted, and the brown residue was rinsed with hexanes (2 × 0.5 mL) and dried under vacuum, yielding the title compound as iridescent bronze flakes. Yield: 55.6 mg (80%). Anal. Calcd for $C_{28}H_{29}N_2O_2W$: C, 55.25; H, 4.80; N, 4.60. Found: C, 55.63; H, 4.96; N, 4.32. IR (THF solution): 1879, 1781 cm^{-1}. ^1H NMR (THF-d_8): δ 8.53 (*m*-H, 4 H, br, 44 Hz), 7.60 (*p*-Me, 6 H, br, 38 Hz), 1.92 (*o*-Me, 12 H, br, 150 Hz), 0.79 (Cp, 5 H, br, 220 Hz). ^1H NMR (toluene-d_8): δ

23.17 (vinyl, 2 H, br, 300 Hz), 8.36 (*m*-H, 4 H, br, 43.2 Hz), 7.56 (*p*-Me, 6 H, br, 37.1 Hz), 1.84 (*o*-Me, 12 H, br, ~200 Hz overlapped), ~1.3 (Cp, 5 H, br, ~50 Hz, overlapped).

Line Shape Analysis of Degenerate Electron Transfer between $CpW(CO)_2(IMes)^\bullet$ and $[CpW(CO)_2(IMes)]^-[K(18\text{-crown-6})]^+$. Stock solutions of $CpW(CO)_2(IMes)^\bullet$ (14.0 mg, 23.0 μmol) and $[CpW(CO)_2(IMes)]^-[K(18\text{-crown-6})]^+$ (21.9 mg, 24.0 μmol) in THF-d_8 (2.00 mL for each) were prepared. For each solution, the total organotungsten concentration was determined by dissolving triphenylmethylsilane (10.1 mg, 36.8 μmol) in 0.50 mL of the stock solution, followed by integration of organotungsten ^{1}H NMR resonances vs triphenylmethylsilane. Measured concentrations were 8.08 mM for $CpW(CO)_2(IMes)^\bullet$ and 12.8 mM for $[CpW(CO)_2(IMes)]^-[K(18\text{-crown-6})]^+$. Samples of varying composition were prepared using the stock solutions, by combining $n \times 0.1$ mL of $CpW(CO)_2(IMes)^\bullet$ solution with $(5 - n) \times 0.1$ mL of $[CpW(CO)_2(IMes)]^-[K(18\text{-crown-6})]^+$ solution (n = 1, 2, 3, 4). Spectra were acquired at 20 °C using 16 scans with a relaxation delay of 1.0 s. Data were imported into gNMR for full line shape analysis. Spectra of isolated $CpW(CO)_2(IMes)^\bullet$ in THF-d_8 and $[CpW(CO)_2(IMes)]^-[K(18\text{-crown-6})]^+$ in THF-d_8 (with NaK added to remove any radical impurity) were employed to represent zero-exchange-limit data. For line fitting, original spectra of the mixtures were partitioned to facilitate computation, with *m*-H and *p*-Me signals grouped in one partition and *o*-Me and Cp signals in another. Vinyl resonances were observed to broaden into the baseline and were not modeled. Refinements converged well, with residual mean square differences on the order of 1×10^{-7} or better in all cases. The rate constant was taken as the average over all line fits according to the rate law shown in eq 7.

$$v_{exchange} = k_{exchange}[CpW(CO)_2(IMes)^\bullet][CpW(CO)_2(IMes)^-] \quad (7)$$

No correction was made for possible concentration-dependent ion-pairing effects in the tungsten anion or for disproportionation in the radical, and no systematic error was evidenced in the calculated rate constants. The rate constant for this process is $1.2(7) \times 10^6$ M^{-1} s^{-1}, with error provided at the 2σ confidence level.

Computational Details. DFT calculations were carried out using the Gaussian03 set of programs.[66] Geometries were optimized using a hybrid basis set utilizing the B3LYP functional[67] or the ROB3LYP treatment[68] for radicals together with the CEP-121G basis set and ECP pseudopotential at W and the 6-31G* basis set for C, H, N, and O. Frequency calculations were used to demonstrate ground states for all species by the absence of imaginary frequencies (geometries exhibit positive eigenvalues). Correction of enthalpies and free energies to 298 K utilized unscaled harmonic frequencies. To estimate W−H and W−W BDEs, single-point calculations were carried out on the above geometries, using the enhanced basis set 6-311++G(2d,2p) for C, H, N, and O atoms and CEP-121G ECP for W.

■ ASSOCIATED CONTENT

Ⓢ Supporting Information. Crystallographically determined W−C_{IMes} bond distances, IR data (*o*-difluorobenzene solution), and reversible oxidation potentials (MeCN, 0.2 M $^nBu_4N^+PF_6^-$) for $CpW(CO)_2(IMes)$ species; simulated and observed EPR spectra at room temperature, 200 K, and 80 K; plots of δ_{iso} vs T^{-1} for the ^{1}H NMR spectra of $CpW(CO)_2(IMes)^\bullet$; graphics showing the computed structures of $CpW(CO)_2(IMes)^\bullet$, $CpW(CO)_2(IMes)H$, $CpW(CO)_2(IMe)^\bullet$, and $CpW(CO)_2(IMes)^\bullet$; comparison between experimental and computational geometric parameters; additional computational details; descriptions of of X-ray structural analyses, and crystallographic data and structure refinement for $[CpW(CO)_2(IMes)]^-[K(18\text{-crown-6})]^+$ and $CpW(CO)_2(IMes)^\bullet$ (including CIF files); complete ref 66. This material is available free of charge via the Internet at http://pubs.acs.org.

■ AUTHOR INFORMATION

Corresponding Author
morris.bullock@pnnl.gov

Notes
[§]Deceased August 12, 2010

■ ACKNOWLEDGMENT

We thank the U.S. Department of Energy, Office of Science, Office of Basic Energy Sciences, Division of Chemical Sciences, Biosciences and Geosciences for support of this work. The low-temperature EPR studies were performed at the William R. Wiley Environmental Molecular Sciences Laboratory (EMSL), a national scientific user facility sponsored by the Department of Energy's Office of Biological and Environmental Research located at PNNL. Provision of high performance computing resources at the National Energy Research Scientific Computing Facility (NERSC) by the Office of Science, U.S. Department of Energy, is gratefully acknowledged. Pacific Northwest National Laboratory is operated by Battelle for the U.S. Department of Energy.

■ REFERENCES

(1) Baird, M. C. *Chem. Rev.* **1988**, *88*, 1217–1227.
(2) Tyler, D. R. *Prog. Inorg. Chem.* **1988**, *36*, 125–194.
(3) Meyer, T. J.; Caspar, J. V. *Chem. Rev.* **1985**, *85*, 187–218.
(4) (a) Stiegman, A. E.; Stieglitz, M.; Tyler, D. R. *J. Am. Chem. Soc.* **1983**, *105*, 6032–6037. (b) Steigman, A. E.; Tyler, D. R. *Coord. Chem. Rev.* **1985**, *63*, 217–240. (c) Tyler, D. R. *Acc. Chem. Res.* **1991**, *24*, 325–331.
(5) Scott, S. L.; Espenson, J. H.; Zhu, Z. *J. Am. Chem. Soc.* **1993**, *115*, 1789–1797.
(6) (a) Scott, S. L.; Espenson, J. H.; Bakac, A. *Organometallics* **1993**, *12*, 1044–1047. (b) Song, J.-S.; Bullock, R. M.; Creutz, C. *J. Am. Chem. Soc.* **1991**, *113*, 9862–9864.
(7) VanVlierberge, B. A.; Abrahamson, H. B. *J. Photochem. Photobiol. A, Chem.* **1990**, *52*, 69–81.
(8) Peters, J.; George, M. W.; Turner, J. J. *Organometallics* **1995**, *14*, 1503–1506.
(9) Virrels, I. G.; George, M. W.; Johnson, F. P. A.; Turner, J. J.; Westwell, J. R. *Organometallics* **1995**, *14*, 5203–5208.
(10) (a) Kling, M. F.; Cahoon, J. F.; Glascoe, E. A.; Shanoski, J. E.; Harris, C. B. *J. Am. Chem. Soc.* **2004**, *126*, 11414–11415. (b) Cahoon, J. F.; Kling, M. F.; Schmatz, S.; Harris, C. B. *J. Am. Chem. Soc.* **2005**, *127*, 12555–12565. (c) Cahoon, J. F.; Kling, M. F.; Sawyer, K. R.; Frei, H.; Harris, C. B. *J. Am. Chem. Soc.* **2006**, *128*, 3152–3153. (d) Cahoon, J. F.; Kling, M. F.; Sawyer, K. R.; Andersen, L. K.; Harris, C. B. *J. Mol. Struct.* **2008**, *890*, 328–338. (e) Baiz, C. R.; McCanne, R.; Kubarych, K. J. *J. Am. Chem. Soc.* **2009**, *131*, 13590–13591. (f) Kania, R.; Stewart, A. I.; Clark, I. P.; Greetham, G. M.; Parker, A. W.; Towrie, M.; Hunt, N. T. *Phys. Chem. Chem. Phys.* **2010**, *12*, 1051–1063.
(11) Pugh, J. R.; Meyer, T. J. *J. Am. Chem. Soc.* **1992**, *114*, 3784–3792.
(12) Fei, M.; Sur, S. K.; Tyler, D. R. *Organometallics* **1991**, *10*, 419–423.
(13) McLain, S. J. *J. Am. Chem. Soc.* **1988**, *110*, 643–644.
(14) Watkins, W. C.; Jaeger, T. J.; Kidd, C. E.; Fortier, S.; Baird, M. C.; Kiss, G.; Roper, G. C.; Hoff, C. D. *J. Am. Chem. Soc.* **1992**, *114*, 907–914.
(15) Yao, Q.; Bakac, A.; Espenson, J. H. *Organometallics* **1993**, *12*, 2010–2012.

(16) For leading references to persistent free radicals, see: (a) Griller, D.; Ingold, K. U. *Acc. Chem. Res.* **1976**, *9*, 13–19. (b) Daikh, B. E.; Finke, R. G. *J. Am. Chem. Soc.* **1992**, *114*, 2938–2943. (c) Bravo, A.; Bjorsvik, H.-R.; Fontana, F.; Liguori, L.; Minisci, F. *J. Org. Chem.* **1997**, *62*, 3849–3857. (d) Fischer, H. *Chem. Rev.* **2001**, *101*, 3581–3610. (e) Focsaneanu, K.-S.; Scaiano, J. C. *Helv. Chim. Acta* **2006**, *89*, 2473–2482. (f) Fischer, H. *Macromolecules* **1997**, *30*, 5666–5672. (g) Fischer, H. *J. Am. Chem. Soc.* **1986**, *108*, 3925–3927.

(17) (a) Hartung, J.; Pulling, M. E.; Smith, D. M.; Yang, D. X.; Norton, J. R. *Tetrahedron* **2008**, *64*, 11822–11830. (b) Choi, J.; Tang, L.; Norton, J. R. *J. Am. Chem. Soc.* **2007**, *129*, 234–240. (c) Tang, L.; Papish, E. T.; Abramo, G. P.; Norton, J. R.; Baik, M.-H.; Friesner, R. A.; Rappé, A. *J. Am. Chem. Soc.* **2003**, *125*, 10093–10102.

(18) Cooley, N. A.; Watson, K. A.; Fortier, S.; Baird, M. C. *Organometallics* **1986**, *5*, 2563–2565.

(19) Philipp, C. C.; White, P. S.; Templeton, J. L. *Inorg. Chem.* **1992**, *31*, 3825–3830.

(20) Lang, R. F.; Ju, T. D.; Kiss, G.; Hoff, C. D.; Bryan, J. C.; Kubas, G. J. *J. Am. Chem. Soc.* **1994**, *116*, 7917–7918.

(21) Adams, C. J.; Bartlett, I. M.; Boonyuen, S.; Connelly, N. G.; Harding, D. J.; Hayward, O. D.; McInnes, E. J. L.; Orpen, A. G.; Quayle, M. J.; Rieger, P. H. *Dalton Trans.* **2006**, 3466–3477.

(22) Pleune, B.; Morales, D.; Meunier-Prest, R.; Richard, P.; Collange, E.; Fettinger, J. C.; Poli, R. *J. Am. Chem. Soc.* **1999**, *121*, 2209–2225.

(23) van der Eide, E. F.; Piers, W. E.; Parvez, M.; McDonald, R. *Inorg. Chem.* **2007**, *46*, 14–21.

(24) Lindsell, W. E. *J. Chem. Soc., Dalton Trans.* **1975**, 2548–2552.

(25) Johnson, M. K.; Rees, D. C.; Adams, M. W. W. *Chem. Rev.* **1996**, *96*, 2817–2840.

(26) (a) Dröge, T.; Glorius, F. *Angew. Chem., Int. Ed.* **2010**, *49*, 6490–6952. (b) Díez-González, S.; Marion, N.; Nolan, S. P. *Chem. Rev.* **2009**, *109*, 3612–3676. (c) Herrmann, W. A. *Angew. Chem., Int. Ed.* **2002**, *41*, 1290–1309. (d) Bourissou, D.; Guerret, O.; Gabbaï, F. P.; Bertrand, G. *Chem. Rev.* **2000**, *100*, 39–91. (e) Herrmann, W. A.; Köcher, C. *Angew. Chem., Int. Ed. Engl.* **1997**, *36*, 2162–2187.

(27) (a) Danopoulos, A. A.; Tsoureas, N.; Wright, J. A.; Light, M. E. *Organometallics* **2003**, *23*, 166–168. (b) Danopoulos, A.A.; Pugh, D.; Smith, H.; Sassmannshausen, J. *Chem.—Eur. J.* **2009**, *15*, 5491–5502.

(28) Danopoulos, A. A.; Wright, J. A.; Motherwell, W. B.; Ellwood, S. *Organometallics* **2004**, *23*, 4807–4810.

(29) Pugh, D.; Wright, J. A.; Freeman, S.; Danopoulos, A. A. *Dalton Trans.* **2006**, 775–782.

(30) Hu, X.; Castro-Rodriguez, I.; Meyer, K. *Chem. Commun.* **2004**, 2164–2165.

(31) (a) Hu, X.; Castro-Rodriguez, I.; Meyer, K. *J. Am. Chem. Soc.* **2004**, *126*, 13464–13473. (b) Hu, X.; Meyer, K. *J. Am. Chem. Soc.* **2004**, *126*, 16322–16323.

(32) Hu, X.; Castro-Rodriguez, I.; Meyer, K. *J. Am. Chem. Soc.* **2003**, *125*, 12237–12245.

(33) Chen, C.; Qiu, H.; Chen, W.; Wang, D. *J. Organomet. Chem.* **2008**, *693*, 3273–3280.

(34) Tumanskii, B.; Sheberla, D.; Molev, G.; Apeloig, Y. *Angew. Chem., Int. Ed.* **2007**, *46*, 7408–7411.

(35) Lorber, C.; Vendier, L. *Organometallics* **2008**, *27*, 2774–2783.

(36) Lorber, C.; Vendier, L. *Dalton Trans.* **2009**, 6972–6984.

(37) Abernethy, C. D.; Cowley, A. H.; Jones, R. A.; Macdonald, C. L. B.; Shukla, P.; Thompson, L. K. *Organometallics* **2001**, *20*, 3629–3631.

(38) Liu, T.; Darensbourg, M. Y. *J. Am. Chem. Soc.* **2007**, *129*, 7008–7009.

(39) Ito, M.; Matsumoto, T.; Tatsumi, K. *Inorg. Chem.* **2009**, *48*, 2215–2223.

(40) (a) Abdur-Rashid, K.; Gusev, D. G.; Landau, S. E.; Lough, A. J.; Morris, R. H. *J. Am. Chem. Soc.* **1998**, *120*, 11826–11827. (b) Gusev, D. G.; Lough, A. J.; Morris, R. H. *J. Am. Chem. Soc.* **1998**, *120*, 13138–13147. (c) Abdur-Rashid, K.; Gusev, D. G.; Lough, A. J.; Morris, R. H. *Organometallics* **2000**, *19*, 834–843. (d) Landau, S. E.; Groh, K. E.; Lough, A. J.; Morris, R. H. *Inorg. Chem.* **2002**, *41*, 2995–3007. (e) Hinman, J. G.; Lough, A. J.; Morris, R. H. *Inorg. Chem.* **2007**, *46*, 4392–4401.

(41) Gusev, D. G.; Lough, A. J.; Morris, R. H. *J. Am. Chem. Soc.* **1998**, *120*, 13138–13147.

(42) Kotyk, M. W.; Gorelsky, S. I.; Conrad, J. C.; Carra, C.; Fogg, D. E. *Organometallics* **2009**, *28*, 5424–5431.

(43) (a) Lee, J. P.; Ke, Z.; Ramírez, M. A.; Gunnoe, T. B.; Cundari, T. R.; Boyle, P. D.; Petersen, J. L. *Organometallics* **2009**, *28*, 1758–1775. (b) Ritleng, V.; Barth, C.; Brenner, E.; Milosevic, S.; Chetcuti, M. J. *Organometallics* **2008**, *27*, 4223–4228.

(44) Moore, E. J.; Sullivan, J. M.; Norton, J. R. *J. Am. Chem. Soc.* **1986**, *108*, 2257–2263.

(45) Roberts, J. A. S.; Appel, A. M.; DuBois, D. L.; Bullock, R. M. *J. Am. Chem. Soc.* **2011**, *133*, No. http://dx.doi.org/10.1021/ja202830w (following paper in this issue).

(46) Roberts, J. A. S.; DuBois, D. L.; Bullock, R. M. *Organometallics* **2011**, published ASAP August 8, 2011 (http://dx.doi.org/10.1021/om2002816).

(47) Wu, F.; Dioumaev, V. K.; Szalda, D. J.; Hanson, J.; Bullock, R. M. *Organometallics* **2007**, *26*, 5079–5090.

(48) Fischer, P. J.; Heerboth, A. P.; Herm, Z. R.; Kucera, B. E. *Organometallics* **2007**, *26*, 6669–6673.

(49) (a) Cheng, T.-Y.; Brunschwig, B. S.; Bullock, R. M. *J. Am. Chem. Soc.* **1998**, *120*, 13121–13137. (b) Cheng, T.-Y.; Bullock, R. M. *J. Am. Chem. Soc.* **1999**, *121*, 3150–3155. (c) Cheng, T.-Y.; Bullock, R. M. *Organometallics* **2002**, *21*, 2325–2331.

(50) Beck, W.; Sünkel, K. *Chem. Rev.* **1988**, *88*, 1405–1421.

(51) Dioumaev, V. K.; Szalda, D. J.; Hanson, J.; Franz, J. A.; Bullock, R. M. *Chem. Commun.* **2003**, 1670–1671.

(52) Li, S.; Kee, C. W.; Huang, K.-W.; Hor, T. S. A.; Zhao, J. *Organometallics* **2010**, *29*, 1924–1933.

(53) Macchioni, A. *Chem. Rev.* **2005**, *105*, 2039–2074.

(54) Darensbourg, M. Y. *Prog. Inorg. Chem.* **1985**, *33*, 221–274.

(55) (a) Tilset, M.; Parker, V. D. *J. Am. Chem. Soc.* **1989**, *111*, 6711–6717. *J. Am. Chem. Soc.* **1990**, *112*, 2843. (b) Kadish, K. M.; Lacombe, D. A.; Anderson, J. E. *Inorg. Chem.* **1986**, *25*, 2246–2250.

(56) Rieger, P. H. *Coord. Chem. Rev.* **1994**, *135/136*, 203–286.

(57) (a) Fortier, S.; Baird, M. C.; Preston, K. F.; Morton, J. R.; Ziegler, T.; Jaeger, T. J.; Watkins, W. C.; MacNeil, J. H.; Watson, K. A.; Hensel, K.; Le Page, Y.; Charland, J.-P.; Williams, A. J. *J. Am. Chem. Soc.* **1991**, *113*, 542–551. (b) MacNeil, J. H.; Roszak, A. W.; Baird, M. C.; Preston, K. F.; Rheingold, A. L. *Organometallics* **1993**, 4402–4412.

(58) Paul, F.; da Costa, G.; Bondon, A.; Gauthier, N.; Sinbandhit, S.; Toupet, L.; Costuas, K.; Halet, J.-F.; Lapinte, C. *Organometallics* **2007**, *26*, 874–896.

(59) Protasiewicz, J. D.; Theopold, K. H. *J. Am. Chem. Soc.* **1993**, *115*, 5559–5569.

(60) Woska, D. C.; Ni, Y.; Wayland, B. B. *Inorg. Chem.* **1999**, *38*, 4135–4138.

(61) Capps, K. B.; Bauer, A.; Kiss, G.; Hoff, C. D. *J. Organomet. Chem.* **1999**, *586*, 23–30.

(62) Wayland, B. B.; Ba, S.; Sherry, A. E. *Inorg. Chem.* **1992**, *31*, 148–150.

(63) Wayland, B. B.; Ba, S.; Sherry, A. E. *J. Am. Chem. Soc.* **1991**, *113*, 5305–5311.

(64) Wayner, D. D. M.; Parker, V. D. *Acc. Chem. Res.* **1993**, *26*, 287–294.

(65) Budzelaar, P. H. M. *gNMR*,v. 5.0.6.0; IvorySoft, 2006.

(66) Frisch, M. J.; et al. *Gaussian 03*, Revision D.02; Gaussian, Inc.: Wallingford, CT, 2004.

(67) (a) Becke, A. D. *J. Chem. Phys.* **1993**, *98*, 5648–5652. (b) Lee, C. T.; Yang, W. T.; Parr, R. G. *Phys. Rev. B* **1988**, *37*, 785–789.

(68) (a) Krishnan, R.; Binkley, J. S.; Seeger, R.; Pople, J. A. *J. Chem. Phys.* **1980**, *72*, 650–654. (b) Blaudeau, J.-P.; McGrath, M. P.; Curtiss, L. A.; Radom, L. *J. Chem. Phys.* **1997**, *107*, 5016–5021. (c) Clark, T.; Chandrasekhar, J.; Spitznagel, G. W.; Von Ragué Schleyer, P. *J. Comput. Chem.* **1983**, *4*, 294–301.